Available online at www.sciencedirect.com
ScienceDirect
Plant Science 173 (2007) 358–369
PLANT SCIENCE
www.elsevier.com/locate/plantsci

Isolation and characterization of *ZePES* and *AtPES*, the *pescadillo* orthologs from *Zinnia* and *Arabidopsis*

Aris Zografidis [a], Georgios Kapolas [a], Georgios Kitsios [b], Maureen McCann [c], Keith Roberts [d], Dimitra Milioni [b], Kosmas Haralampidis [a,*]

[a] *University of Athens, Faculty of Biology, Department of Botany, 15784 Athens, Greece*
[b] *Agricultural University of Athens, Department of Agricultural Biotechnology, Iera Odos 75, 11855 Athens, Greece*
[c] *Department of Biological Sciences, Purdue University, West Lafayette, IN 47907-1392, USA*
[d] *John Innes Centre, Norwich Research Park, Colney, Norwich NR4 7UH, UK*

Received 4 May 2007; received in revised form 20 June 2007; accepted 26 June 2007
Available online 3 July 2007

Abstract

The *pescadillo* gene was originally identified and characterized through a mutational screen in zebrafish, *Danio rerio*, affecting embryonic development. Subsequent reports have shown that the yeast and animal homologs are implicated in ribosome biogenesis, cell cycle progression and carcinogenesis, while disruption of its function leads to growth arrest. At present, no orthologs of the pescadillo gene have been characterized in plants. Here we report, for the first time, the isolation and characterization of the *pescadillo* orthologs from *Zinnia elegans* (*ZePES*) and *Arabidopsis thaliana* (*AtPES*). *ZePES*, which is expressed differentially throughout tracheary element differentiation of *Zinnia* mesophyll cells, is upregulated during G1/S and G2/M transition. Both *ZePES* and *AtPES* are able to complement the temperature-sensitive phenotype of yeast degron strain Y40047, impaired in the *NOP7/YPH1* gene (*pescadillo* ortholog), indicating a functional conservation between the yeast and plant gene products. We also show that AtPES–GFP fusion protein is localized in the nucleolus of plant cells. Analysis of transgenic plants reveals that *AtPES* is expressed during vegetative and reproductive development predominantly in meristematic tissues and actively dividing cells, while overexpression of *AtPES* does not lead to any phenotypic changes during growth and development.

Keywords: β-Glucuronidase; GFP; Nucleolus; *Pescadillo*; Yeast complementation; *Zinnia*

1. Introduction

The *pescadillo* gene (*pes*) was initially isolated by Allende et al. [1], who showed that normal development in zebrafish (*Danio rerio*) requires expression of *pescadillo* in a number of tissues, including the eyes and optic tectum, the fin buds, liver primordium and the branchial arches. Pescadillo$^{-/-}$ zebrafish mutants exhibit a lethal phenotype since embryos die on the sixth day of development due to severe defects in numerous organs [1]. Subsequently, *pescadillo* homologs were identified and characterized from mouse (*Pes1*), human (*PES1*) and yeast (*NOP7/YPH1*) [2–4]. Pescadillo is a strongly conserved protein containing unique structural motifs: a BRCT-1 domain (breast cancer carboxy-terminal domain) and two consensus motifs for post-translational modification by SUMO-1. The BRCT-1 domain, first identified in the breast cancer suppressor protein BRCA1, is an evolutionarily conserved protein–protein interaction region, found in a large number of proteins involved in DNA repair, recombination and cell cycle control [5–7]. The consequences of SUMO-1 modification include the regulation of protein–protein interactions, protein–DNA interactions, and protein subcellular localization [8–10].

All *pescadillo* homologs characterized to date are localized in the nucleolus, while in mouse Lerch-Gaggl et al. [11] have shown that Pescadillo (Pes1) is also associated with the chromosome periphery, nucleolus-derived foci and prenucleolar bodies during mitosis. They also demonstrated that loss of Pes1 function results in embryonic lethality due to a disruption in ribosome biogenesis. The authors therefore concluded that Pes1 is essential for nucleolar assembly and is an integral

* Corresponding author at: University of Athens, Faculty of Biology, Department of Botany, Laboratory of Physiology and Molecular Plant Development, 15784 Athens, Greece Tel.: +30 210 7274131; fax: +30 210 7274702.
E-mail address: kharalamp@biol.uoa.gr (K. Haralampidis).

0168-9452/$ – see front matter
doi:10.1016/j.plantsci.2007.06.009

component of the ribosome-generating machinery. More recently, Lapik et al. [12] have shown that Pes1 physically interacts with the nucleolar protein Bop1, and that both proteins direct common pre-rRNA processing steps. *Pes1* mutants defective for the interaction with Bop1 lose the ability to affect rRNA maturation and the cell cycle [12]. The involvement of Pescadillo in ribosome biogenesis and in the regulation of cell growth has also been shown in yeast [4,13]. Temperature-sensitive Nop7/Yph1 yeast mutant strains (containing a single point mutation in the BRCT domain) displayed growth arrest in the G1 or G2 phase of the cell cycle when shifted to a non-permissive temperature [3,14].

These data confirmed that Pescadillo is required for cell cycle progression and pointed out the importance of the BRCT domain in Pescadillo activity. Cell cycle progression and consequently cell proliferation requires cell growth and DNA synthesis. Cell growth however is dependent on ribosome biogenesis and protein synthesis. It makes sense, therefore, that there should be some cross-talk between those programs, with Pescadillo being an attractive possibility for a link between cell division and increase in cell size. Such a link between cell proliferation control, DNA replication and ribosome biogenesis has been reported by Du and Stillman [14], who showed immunoprecipitation of Nop7/Yph1 along with the origin recognition complex (ORC). Consistent with this hypothesis, Killian et al. [15] have demonstrated that alteration of proteins linking ribosome biogenesis and DNA replication may directly cause chromosomal instability and cell death. Furthermore, a number of interesting reports provide evidence for a link between Pescadillo and carcinogenesis. Although Pescadillo is not itself directly oncogenic [3,16,17], its expression is often upregulated in cancer cells [18]. Recently, a previously unrecognized role has been assigned to Pescadillo by Sikorski et al. [19], who showed that it can function as a DNA-binding protein interacting specifically with the cadmium response element of the human heme oxygenase-1 gene.

Nevertheless, plant orthologs of the *pescadillo* gene have not been characterized to date. In the present study, we report the molecular cloning and characterization of the *pescadillo* orthologs from *Zinnia elegans* (*ZePES*) and *Arabidopsis thaliana* (*AtPES*). We show that *AtPES* encodes a nucleolar protein and that both orthologs are able to complement the Y40047 yeast degron strain impaired in the *NOP7/YPH1* gene (*pescadillo* ortholog). Analysis of promoter-GUS transgenic plants demonstrates that *AtPES* is predominantly upregulated in proliferating cell types and actively dividing cells, while ectopic expression of *AtPES* did not result in any obvious abnormal phenotypes.

2. Materials and methods

2.1. Plant material and growth conditions

Wild-type and transgenic *A. thaliana* (Col) plants were grown under standard conditions at 22 °C in 70% humidity with a light/dark cycle of 16 h/8 h and illumination of 110 μmol/m^2 s PAR supplied by cool-white fluorescent tungsten tubes (Osram, Germany). Seeds from individual T2 or T3 transgenic plants were imbibed at 4 °C overnight, and were surface-sterilized for 2 min with 70% (v/v) ethanol and for 5 min with 15% (v/v) sodium hypochlorite containing 0.1% (v/v) Tween 20. After several washing steps with sterile deionized water, seeds were germinated on Murashige and Skoog medium containing 50 mg/L kanamycin and 200 mg/L cefotaxime under the same growth conditions. Transgenic plants were transferred to soil for further development. Cell suspension cultures from *A. thaliana* ecotype Col-1 were established and maintained as described elsewhere [20].

Mesophyll cells from 2-week-old *Z. elegans* plants were isolated and cultured as described by Domingo et al. [21] using medium with no growth factors, 1 mg/L benzylaminopurine and 1 mg/L naphthalene acetic acid (inductive medium), 1 mg/L benzylaminopurine alone, or 1 mg/L naphthalene acetic acid alone. Cells were transferred from non-inductive to inductive media at 48 h from the wells in six-well plates into 30-mL screw-cap tubes (Bibby Sterilin, Stone, UK); the tubes were centrifuged at 800 rpm for 2 min, and the cells were gently suspended in new medium at density of 106 cells/mL.

2.2. DNA sequence analysis

DNA was sequenced by the dideoxy chain termination method with use of an automated sequencer model 377 (Applied Biosystems).

2.3. Computational analysis and phylogenetic tree construction

Analysis of the DNA and protein sequences was performed using the Basic Local Alignment Search Tool (BLAST) and the Conserved Domain Database (CDD) at NCBI. Potential subcelullar localization of the proteins was predicted by use of PSORT (http://www.psort.org/) and LOCtree (http://cubic.bioc.columbia.edu/). Full-length amino acid sequences were downloaded from http://www.ncbi.nml.nih.gov/ and aligned by CLUSTALW at EBI (http://www.ebi.ac.uk/clustalw/). The phylogenetic tree was constructed by using the neighbour-joining method as implemented in the NEIGHBOR program of the PHYLIP package, version 3.65 (Department of Genome Science, University of Washington, Seatle, WA, USA). Amino acid distances were calculated by using the Dayhoff PAM matrix method of the PROTDIST program of PHYLIP. The statistical significance was tested by bootstrap analysis for 1000 replicates. The final tree was visualized using TreeView 1.6.6. The numbers indicate the bootstrap replications (of 1000) in which the given branching was observed. The protein parsimony method (the PROTPARS program of PHYLIP) produced trees with essentially identical topologies.

2.4. RACE-PCR and cloning of ZePES

Rapid Amplification of mRNA Ends by PCR (RACE-RCR) was performed according to the manufacturer's protocol, using the Marathon cDNA Amplification Kit (Clontech).

Gene-specific primers were synthesized based on a previously characterized sequence of a 218-bp cDNA-AFLP fragment. Primer sequences for the first round of PCR were: for 5′-RACE Zpes51 (5′-GACCTTCTTCTCGTATGCTCGCATCTCACG-GA-3′) and for 3′-RACE Zpes31 (5′-GCTGAACGCTTGTT-GACAAGAAAGCCTACTTA-3′). PCR conditions were: 94 °C for 1 min, followed by five cycles of 94 °C for 30 s, 72 °C for 4 min, followed by five cycles of 94 °C for 30 s, 70 °C for 4 min, followed by 25 cycles of 94 °C for 30 s, 68 °C for 4 min. A second round of PCR with nested primers was performed on 1:200 dilutions of the primary PCR reaction products. The gene-specific primers for the second round were: for 5′-RACE Zpes52 (5′-ACGGAATTTATCAAGAAGTGGCTCATG-3′) and for 3′-RACE Zpes32 (5′-TACACTCTTGATATGCT-TATCCGGGAGAG-3′). Adaptor primers were also nested for this second round. Conditions were as in the first round except the last set of cycles was 18 instead of 25. The 5′ and 3′-RACE products were purified, subcloned and sequenced. The primer pair Zpes53 (5′-ATGCCGAAGCACTACAGACCT-CCTG-3′) and Zpes33 (5′-TCAATCTGATGACTTTTTCT-TGTTTTTTTG-3′) were subsequently used in order to amplify and clone the entire *ZePES* cDNA (GenBank accession no. AM418533).

2.5. Semi-quantitative RT-PCR

Total RNA was extracted from *Z. elegans* and *A. thaliana* samples with the RNeasy Plant Kit (Qiagen). Two micrograms of total RNA was treated with 20 U DNase I (Roche Applied Science) for 10 min at 37 °C. First strand cDNA was synthesized from 1 μg total RNA in a volume of 20 μL with Expand Reverse Transcriptase (50 U/μL, Roche) according to the manufacturer's protocol. Initial PCR was performed in a mixture of 50 μL that contained 1 μL of first-strand cDNA, 10 pmol each of the gene-specific primers, 0,4 mM dNTP's, 1× PCR buffer and 2.5 U Taq DNA Polymerase (Roche). The *ACTIN* gene was used as an internal control for RNA calibration. The volumes of cDNA used as templates for gene amplification were adjusted after preliminary calibration based on the levels of *ACTIN* PCR product. The following thermocycling program was used: initial denaturation at 94 °C for 2 min, followed by the specified number of cycles of 94 °C for 30 s, 60 °C for 30 s, 72 °C for 1 min, and final extension at 72 °C for 5 min. To verify the exponential phase of RT-PCR amplification, 15, 20, 25 and 30 cycles were tested for each gene, and data was collected at 20 cycles for *ACTIN* and at 25 cycles for all other genes. All experiments were performed in triplicate. Primers were as follows: for *ZeH4*, 5′-TCTTTAGAGCATAAACAACGTCCA-TAGCAGTC-3′ and 5′-GGGCGTGGAAAGGGCGGCAAAG-GGGATTAGG-3′; for *ZeCYCB1*, 5′-GACATAACTGCC-AAGATGAGGGCGATTCTAA-3′ and 5′-GCCCAAACT-TCCTCGTACTTTGAGGCAATGAG-3′; for *ZeCDC48*, 5′-CCAAGGGAGGAACAAGTCTTG-3′ and 5′-ATGTTGATCT-TCGTGCCCTTG-3′; for *ZePES*, 5′-ATGCCGAAGCA(C/T)TACAGAC-3′ and 5′-CTCTTGTTTCTTCATC(C/T)TCTTC-3′; for *AtPES* 5′-TTGACCCCTCATGCAATCCAACAA-3′ and 5′-AGATCCTTGAAGAGTGACTTGC-3′; and for *ACTIN* 5′-GTGACAATGGAACCGGAATGGTTAAGGCTGGAT-3′ and 5′-CAGCTTGGATAGCGACATACATGGCAGGAGT-3′.

2.6. Functional complementation of Saccharomyces cerevisiae degron strain

The degron strain Y40047, containing the "heat-inducible degron cassette" at the N terminus of the YGR103w ORF locus (*NOP7/YPH1* gene), was obtained from the EUROSCARF consortium (http://web.uni-frankfurt.de/fb15/mikro/euroscarf/index.html) [22]. For the complementation experiment, the full-length *ZePES* and *AtPES* cDNAs were amplified and cloned into the p416GPD yeast vector [23]. *ZePES* cDNA was amplified by PCR using primer Zpes53 (5′-ATGCCGAAG-CACTACAGACCTCCTG-3′) and Zpes33 (5′-TCAATCTGAT-GACTTTTTCTTGTTTTTTTG-3′) and cloned into the pGEM®-T Easy vector. After verifying the correct orientation of the fragment the clone was digested with restriction enzymes SpeI/EcoRI and the obtained fragment was ligated into the SpeI/EcoRI-linearized p416GPD vector (construct p416ZePES). *AtPES* cDNA was amplified by PCR using primer AtPES-YES5 (5′-TAGGATCCATGCCGAAGCATTA-CAGACCAACGGGGAAA-3′, with an added BamHI site underlined) and AtPES-YES3 (5′-AACTCGAGTCATGAT-GATGGTTGAGTATCATTCAACCT-3′, with an added XhoI site underlined), digested and then ligated into the BamHI/XhoI-linearized p416GPD vector (construct p416AtPES). As a positive control the NOP7/YPH1 cDNA was cloned into the p416GPD vector in a similar manner (construct p416Nop7), using primers Nop7-YESF (5′-TTAGGATCCATGAGAAT-CAAGAAGAAAAACACC-3′) and Nop7-YESR (5′-TTACTCGAGCTATTTCTTGGAATCTAGTTTATTCAG-3′). p416GPD alone was used as a negative control.

Plasmids were transformed into the yeast degron strain Y40047 using standard procedures and Ura+ transformants were selected in glucose SC minus uracil plates. After growth at 25 °C on YPDA plates containing 0.1 mM CuSO4, cells were re-suspended in PBS (optical density at 600 nm [OD_{600}], 0.8). Drops containing 10-fold serial dilutions were subsequently placed on plates under four different conditions: SCGlu at 25 °C; SCGlu at 37 °C; SCGal at 25 °C; SCGal at 37 °C. The plates were incubated for 48–72 h before examination.

2.7. Plasmid construction and plant transformation

For the promoter::*GUS* construct a 572 bp fragment, representing the 5′ regulator region of the *A. thaliana pescadillo* ortholog (accession no. AL163792, At5g14520), was PCR amplified from genomic DNA using primer pair AtPESpdaF3 (5′-TTCAAGCTTTCTGAAATGGGCACCACGTA-3′) and AtPESpdaR (5′-TTCCTGCAGGGTGAAAACGCCACCA-GAGA-3′). Forward and reverse primers were designed with a HindIII and SalI restriction site on the 5′ and 3′ ends, respectively (underlined). The amplified fragment was digested with both enzymes, and cloned into the HindIII/SalI-linearized pGPTV-Kan binary vector [24]. The resulting construct (named

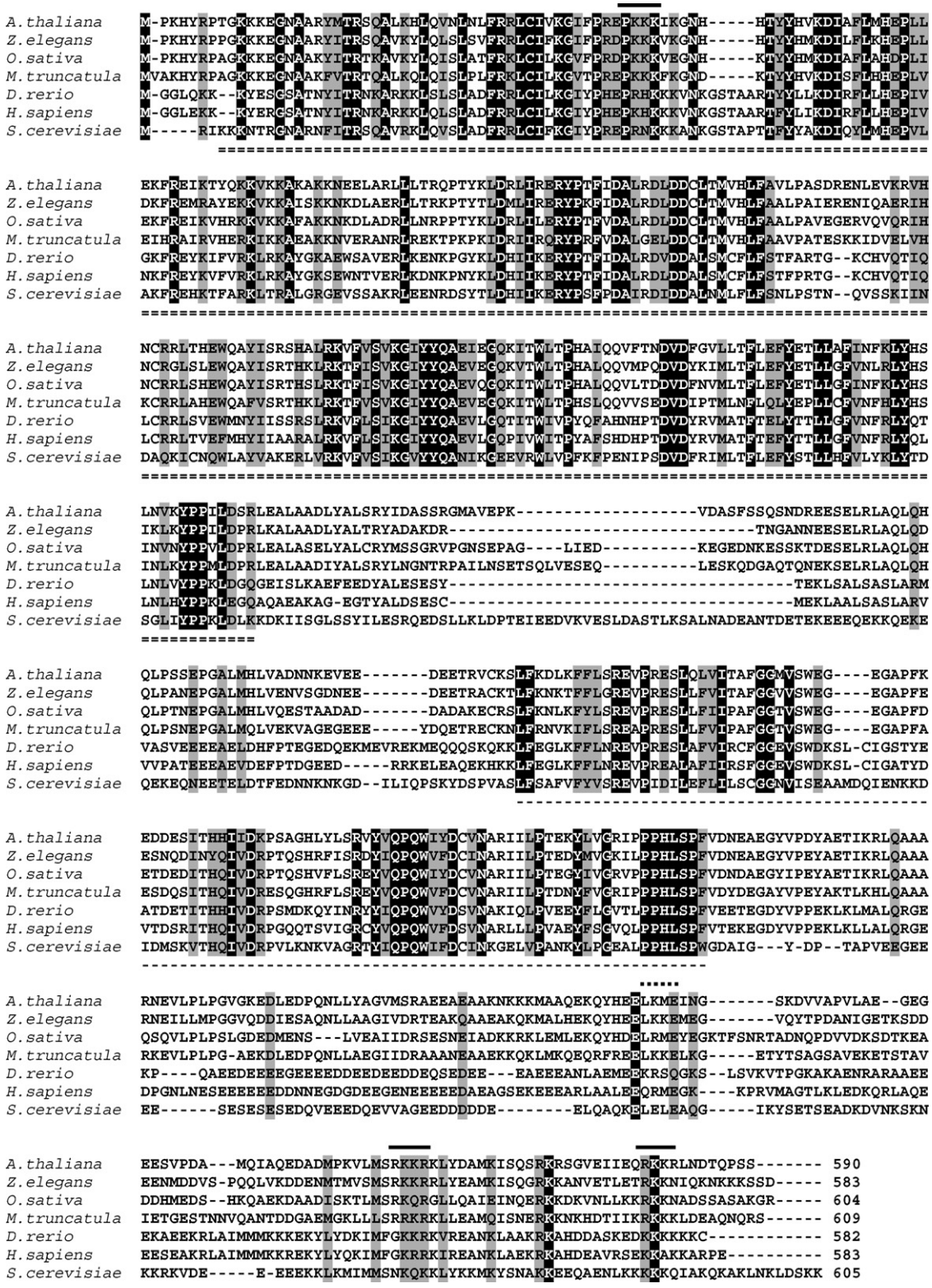

Fig. 1. Alignment of the predicted full-length amino acid sequences of ZePES and AtPES with those of the orthologs from other organisms. Identical and similar residues are shaded in black and grey, respectively. Dashes indicate gaps. Numbers indicate total amino acids of each sequence. The double and single dashed lines below the sequences show the N-terminal pescadillo and the BRCT domain, respectively. The continuous and dashed lines above the sequences indicate the position of the NLS and the SUMO-1 consensus sequence, respectively, found in ZePES and AtPES. *Z. elegans* (*Zinnia elegans*, accession no. AM418533); *A. thaliana* (*Arabidopsis thaliana*, accession no. AL163792); *O. sativa* (*Oryza sativa*, accession no. XP469396); *M. truncatula* (*Medicago truncatula*, accession no. AC125368); *D. rerio* (*Danio rerio*, accession no. NP571105); *H. sapiens* (*Homo sapiens*, accession no. CAG30425); *S. cerevisiae* (*Saccharomyces cerevisiae*, accession no. AAT93034).

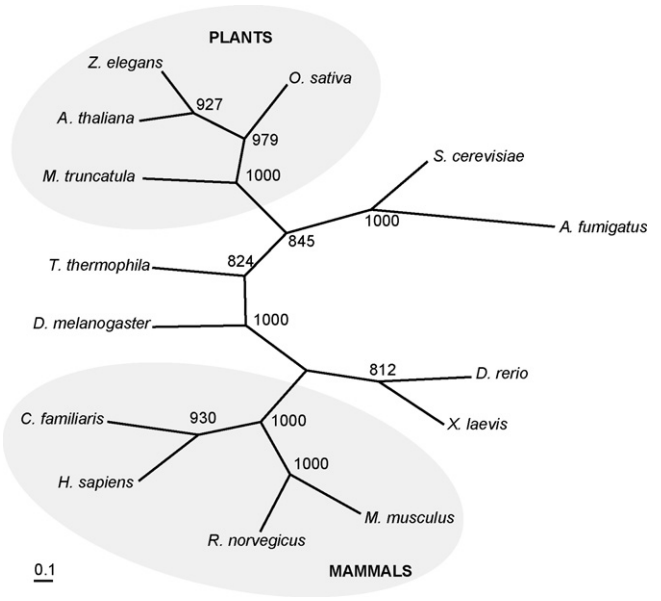

Fig. 2. Phylogenetic analysis of ZePES and AtPES related sequences. A consensus bootstrap neighbour-joining tree based on the CLUSTAL W alignments of the full-length amino acid sequences from different organisms. The bootstrap scores obtained after 1000 bootstrap replicates are indicated at the nodes. Sequences are shown as follows: *Z. elegans* (*Zinnia elegans*, accession no. AM418533); *A. thaliana* (*Arabidopsis thaliana*, accession no. AL163792); *M. truncatula* (*Medicago truncatula*, accession no. AC125368); *O. sativa* (*Oryza sativa*, accession no. XP469396); *X. laevis* (*Xenopus laevis*, accession no. AAH43950); *D. rerio* (*Danio rerio*, accession no. NP571105); *R. norvegicus* (*Rattus norvegicus*, accession no. AAI05911); *M. musculus* (*Mus musculus*, accession no. NP075027); *C. familiaris* (*Canis familiaris*, accession no. XP543480); *H. sapiens* (*Homo sapiens*, accession no. CAG30425); *D. melanogaster* (*Drosophila melanogaster*, accession no. NP609305); *T. thermophila* (*Tetrahymena thermophila*, accession no. EAR99283); *S. cerevisiae* (*Saccharomyces cerevisiae*, accession no. AAT93034); *A. fumigatus* (*Aspergillus fumigatus*, accession no. XP752007).

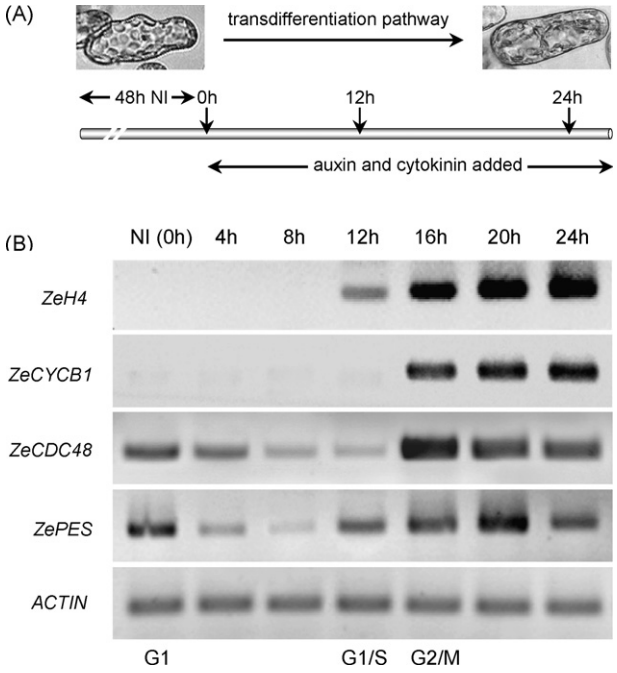

Fig. 3. *ZePES* and cell cycle gene expression during trans-differentiation of *Zinnia* mesophyll cells. (A) Schematic representation of the trans-differentiation time course of Zinnia mesophyll cells into TEs. Isolated cells are maintained for 48 h in non-inductive medium (NI), at which point auxin and cytokinin is added (time point 0 h). (B) RT-PCR gel blots showing the transcript levels of *HISTONE H4* (*ZeH4*), *ZeCYCB1*, *ZeCDC48*, *ZePES* and *ACTIN* from 48 h in NI (0 h) to 24 h after the addition of growth factors. Cell cycle progression as predicted from the transcript profiles is shown at the bottom: G1 (G1 phase), G1/S (G1-to-S phase transition), G2/M (G2-to-M phase transition).

AtPESpro572GUS) was confirmed by restriction enzyme analysis.

For the subcellular localization construct the full-length cDNA of *AtPES* was amplified using primers AtPES-Floc5 (5′-AAGGCGCGCCGATGCCGAAGCATTACAGACCAAC-3′, with an added AscI site) and AtPES-Floc3 (5′-TCGCGGCCGC-TCATGATGATGGTTGAGTATCAT-3′, with an added NotI site), digested and than inserted into the AscI/NotI-linearized pGreenII29+2X35S-GFP-35ST (kindly provided by Nicolas Tsesmetzis) binary vector upstream of the *GFP* gene. The CaMV35S promoter of the above construct was replaced with the 572 bp PCR amplified fragment of the *AtPES* promoter using KpnI and XhoI sites. The resulting construct (named pGPESp-GFP-cAtPES), which contains the translational fusion of *GFP::AtPES* under the native *AtPES* promoter, was confirmed by sequencing.

For generating transgenic lines overexpressing *AtPES*, the entire coding region of the *AtPES* cDNA was amplified using primers oAtPESF (5′-AAGGATCCATGCCGAAGCATTACA-GACCAAC-3′, with an added BamHI site) and oAtPESR (5′-TCGAGCTCTCATGATGATGGTTGAGTATCAT-3′, with an added SacI site), digested and ligated into the BamHI/SacI-linearized pBI121 (Clontech, USA) binary vector, downstream of the CaMV 35S promoter (construct pB35PES). High fidelity DNA polymerases were used for all amplifications.

All binary vector constructs were introduced into the *Agrobacterium tumefaciens* strain GV3101::pGV2260 by the direct transfer method [25]. *Arabidopsis* (*A. thaliana*, L. *erecta*) plants were transformed by using the *in planta A. tumefaciens* vacuum infiltration method as described [26], and seeds from infiltrated plants were germinated on selective (40 mg/L Kanamycin) 0.5× Murashige and Skoog basic medium. Col-1 cell suspension cultures were transformed by *Agrobacterium*, harbouring construct pGPESp-GFP-cAtPES, according to the method described by Mathur et al. [20]. Samples were examined and photographed with an epi-illumination fluorescence microscope (Zeiss, Germany), using a filter set consisting of a blue excitation filter (450–490 nm), a dichroic mirror (510 nm), and a green barrier filter (515–565 nm). Upon request, all constructs and lines described in this article will be made available to the research community.

2.8. Histochemical GUS expression assays

Histochemical staining for GUS activity was performed on the T2 and T3 generation of promoter-GUS plants using 5-bromo-4-chloro-3-indolyl-β-D-glucuronide (X-Gluc) as a substrate [27]. Tissues were stained for 2 h at 37 °C in X-Gluc reaction buffer (50 mM sodium phosphate buffer, pH 7.2,

0.5 mM potassium ferrocyanide, 0.5 mM potassium ferricyanide, and 2 mM X-Gluc), dehydrated by a series of ethanol washes, and kept in 3.7% (w/v) formaldehyde, 50% (w/v) ethanol, and 5% (w/v) acetic acid at 4 °C. Samples were observed and photographed using a stereomicroscope or a differential interference contrast microscope (Olympus, Germany).

3. Results

3.1. Cloning of ZePES and AtPES, sequence analysis and phylogeny

A previously conducted cDNA-AFLP screen, using the *Zinnia* mesophyll cell system, identified 652 differentially accumulated ESTs during the time course of tracheary element (TE) differentiation [28]. Using the Basic Local Alignment Search Tool (BLAST) program against the GenBank non-redundant public sequence database, one of the earliest differentially expressed sequences revealed high identity to the zebrafish *pescadillo* gene. Based on this 218-bp cDNA-AFLP sequence, specific primers were designed in order obtain the 5′ and 3′ end of the cDNA by RACE-RCR. The amplified products were cloned and sequenced to obtain the full-length cDNA contig. Specific primers from the 5′ and 3′ ends were subsequently used to amplify and clone the entire cDNA, named *ZePES* (GenBank accession no. AM418533). Database searches, using the sequence of the cloned *Z. elegans* ortholog, identified one *pescadillo*-like sequence in the *Arabidopsis* genome. We have named this gene, corresponding to loci At5g14520, *AtPES*. Based upon DNA sequence information (AL163792), we designed specific primers to isolate the full-length cDNA of *AtPES* by PCR. DNA sequencing and analysis (BLAST, National Center for Biotechnology Information) of the subcloned PCR product confirmed it as *AtPES*, with complete identity to the full-length sequence deposited in GenBank (AL163792).

The deduced amino acid sequences of the *ZePES* and *AtPES* cDNAs consist of 583 and 590 residues, respectively (Fig. 1). Potential nuclear targeting motifs were found in both sequences, indicating that the proteins are probably localized in the nucleus. The conserved domain search showed that *ZePES* as well as *AtPES* contain one pescadillo N-terminus domain (pfam06732) [11] and one BRCT domain (pfam00533) [5,29]. These two domains are present once in all *pescadillo*-like sequences at similar positions (Fig. 1). Furthermore, motifs for covalent attachment of small ubiquitin-like modifier-1 (SUMO-1) protein were identified at position 509–512

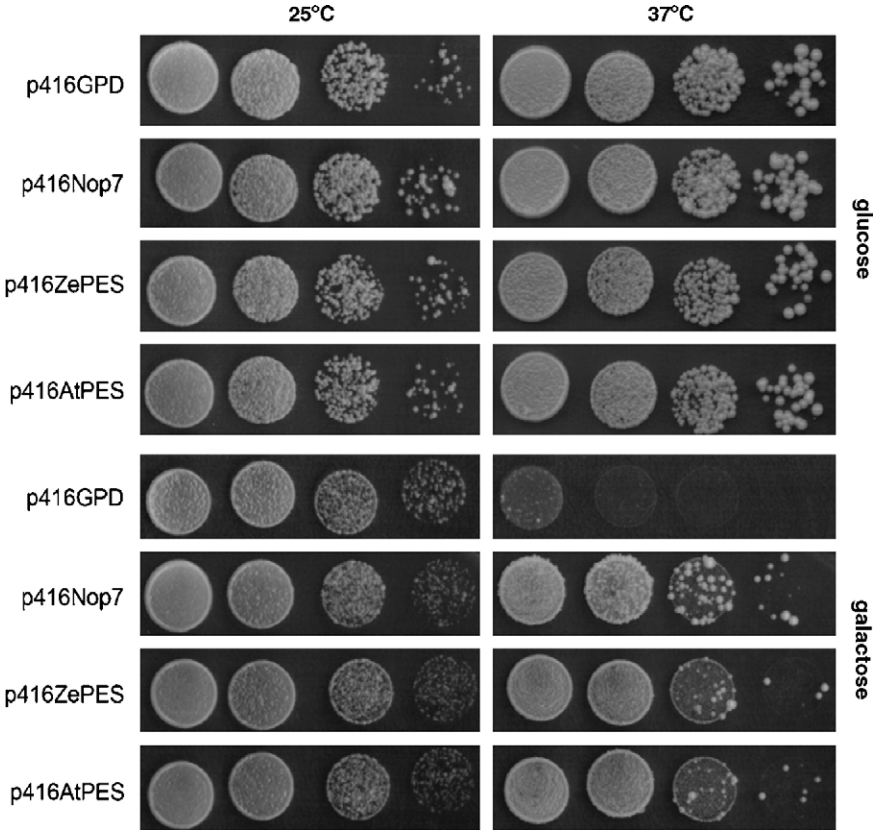

Fig. 4. Complementation of yeast degron strain Y40047 by ZePES and AtPES. Serial dilutions of cells harbouring the *GDP*promoter::*ZePES* (p416ZePES) and *GPD*promoter::*AtPES* (p416AtPES) expression construct were spotted on plates containing glucose or galactose and incubated at the indicated temperatures for 48–72 h. Cells containing construct p416Nop7 and the empty p416GPD vector were used as positive and negative controls, respectively. Yeast cells plated on SCGlu medium either at 25 or 37 °C (*UBR1* OFF), and on SCGal medium at 25 °C (*UBR1* OFF) display normal growth. The degron strain transformed with p416GPD exhibits cell cycle arrest at the non-permissive temperature on SCGal medium (*UBR1* ON). Growth of the degron strain expressing the *NOP7*/*YPH1*, *ZePES* and *AtPES* cDNA, on galactose containing media at 37 °C (*UBR1* ON), indicates complementation.

(LKME) in AtPES and at positions 70–73 (LKHE) and 495–498 (LKKE) in ZePES. These motifs conform to the SUMO-1 consensus sequence (SUMO-1-CS) ΨKXE, where Ψ is a large hydrophobic residue, K is the lysine to which SUMO-1 is conjugated, X is any amino acid and E is glutamic acid [30].

The amino acid identity between ZePES and AtPES is 65%. Both sequences display high identity to the Pescadillo-like sequence from *Oryza sativa* (61 and 62%, respectively) and *Medicago truncatula* (59 and 59%, respectively), and less identity to PES1 of human, Nop7/Yph1 of yeast and Pescadillo of zebrafish (32–38%). The identities mainly occurred in the N-terminal pescadillo domain and the BRCT domain (Fig. 1) along with less identity between their middle linker and the C-terminal regions. Based on the multiple alignments of the full-length amino acid sequences from different organisms a phylogenetic tree was constructed to examine their evolutionary relationship.

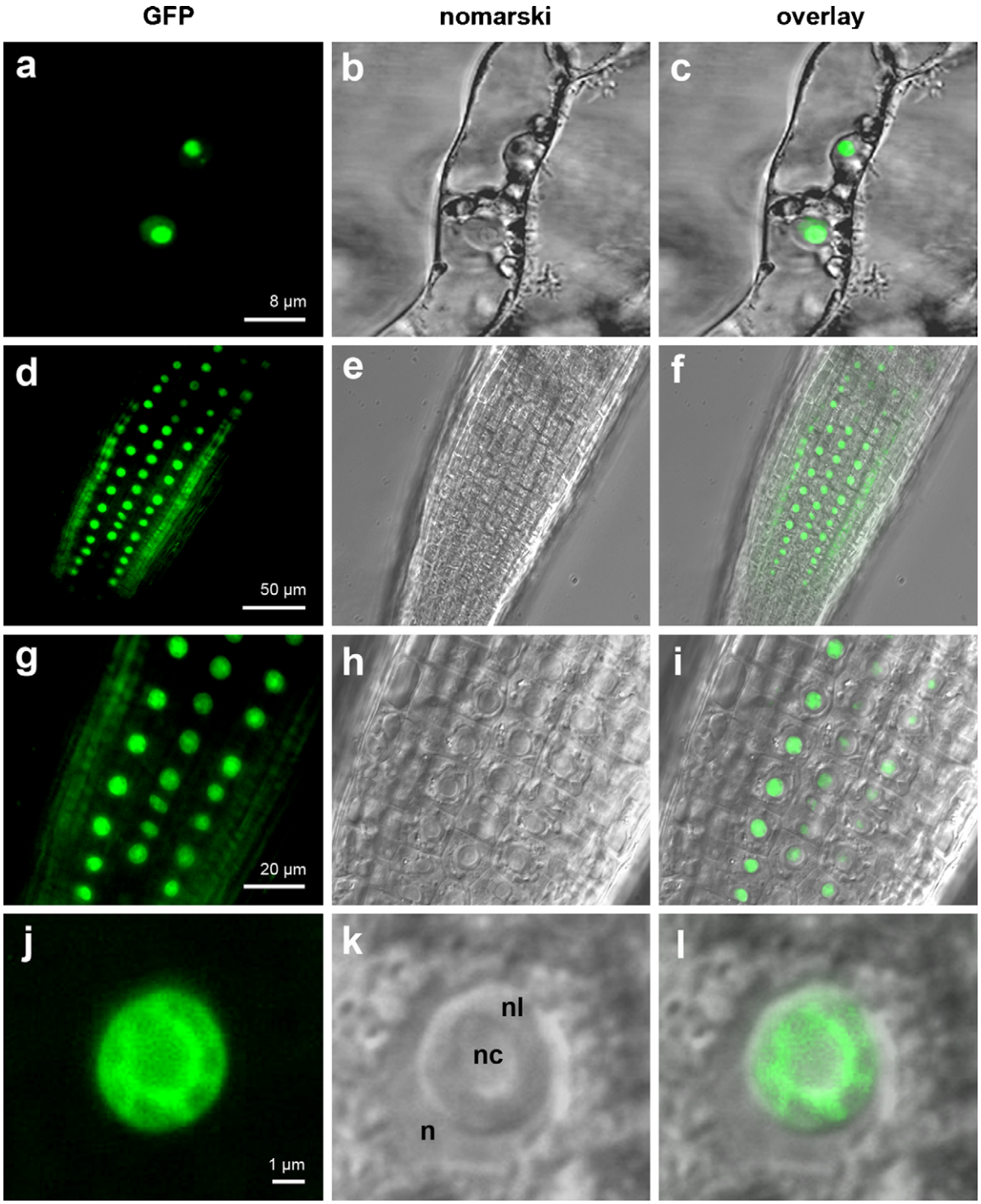

Fig. 5. Subcellular localization of GFP::AtPES. Distribution of the GFP::AtPES fusion protein in *A. thaliana* cell suspension cultures (a–c) and transgenic plants (d–l). Cells were visualized by Nomarski differential interference contrast (DIC) (middle panel) or GFP fluorescence (left panel) on an epifluorescence microscope with filter sets optimal for GFP (Ex 450–490, Dichroic 510, Em 515–565). The fluorescent images were superimposed onto the Nomarski images in the right panel. GFP::AtPES was localized in the nucleolus of plant cells, as the GFP-DIC overlay images show.

As shown in Fig. 2, all plant orthologs cluster together into one group with a high degree of reliability (i.e., in 84.5% of bootstraps). This group forms, together with the lower eukaryotic and insect species a separate clade from the mammalian sequences.

3.2. Expression pattern of ZePES during tracheary element differentiation

ZePES was identified as a differentially accumulated transcript-derived fragment, during an extensive cDNA-AFLP screen on a time course of trans-differentiating *Z. elegans* mesophyll cells to tracheary elements (TEs) [28]. Before differentiating to TEs, almost all cells go through cell division. To study the expression profile of *AtPES* during the first 24 h of trans-differentiation we used a semiquantitative reverse transcription (RT) PCR approach. The expression of cell cycle-regulatory genes was examined in parallel, on reverse transcribed RNA extracted from *Zinnia* cells at 48 h without growth factors (non-inductive medium, NI, time 0) and then at 4, 8, 12, 16, 20 and 24 h after the addition of auxin and cytokinin at time 0. Fig. 3 summarizes the results of the analysis. The G1-to-S transition cell cycle marker gene *HISTONE H4* (*ZeH4*) increased strongly between 12 and 16 h, representing the entry of cells into S phase. Transcripts of the B-type cyclin *ZeCYCB1* (involved in the G2-to-M transition) were undetectable up to time point 12 h, but rose strongly at 16 h. *CDC48*, a G2/M marker gene with an essential role during mitosis, has also been characterized as a critical cell cycle regulator in G1 [31]. Thus, the elevated transcript levels of *ZeCDC48* in NI medium indicate that the majority of the cells are most likely at phase G1. *ZePES* displayed a differential expression pattern during the time course of TE differentiation. Transcripts were high in cells maintained in hormone-free medium (time point 0), but decreased rapidly after the addition of the growth factors to the medium at time point 4 and 8 h. Nevertheless, *ZePES* gene expression increased again both during G1/S (12 h) and G2/M transition (16 h). As calculated by DAPI and Calcofluor staining, the first cell divisions take place 24 h after the addition of auxin and cytokinin to the medium [32]. This observation, which was scored at an average of 47% of living cells, justifies the decrease in *ZePES* gene expression at time point 24 h.

3.3. Yeast complementation

Yeast cells with a complete deletion of the *NOP7/YPH1* open reading frame (YGR103w) display growth arrest in the G1 or G2 phase of the cell cycle when shifted to a non-permissive temperature [3,14]. In view of the amino acid conservation between the Nop7/Yph1, ZePES and AtPES proteins (Fig. 1), especially in the N-terminal pescadillo and BRCT domain, we asked whether the ZePES and AtPES cDNAs can functionally complement the mutant phenotype of the yeast Y40047 strain. Y40047 contains a "heat-inducible degron cassette" at the N terminus of the YGR103w ORF, encoding the Nop7/Yph1 protein. We therefore used a used a *GPD*-promoter-*ZePES* and a *GPD*-promoter-*AtPES* expression construct (p416ZePES and p416AtPES) to complement strain Y40047. Yeast cells transformed with construct p416AtPES, p416Nop7 and with the empty p416GPD vector, were compared for their ability to grow under various conditions. As shown in Fig. 4, cells plated on glucose containing media display normal growth both at 25 and 37 °C (*UBR1* OFF). The degron strain harbouring the empty p416GPD vector also grows normally at 25 °C, on galactose containing media (*UBR1* OFF). However, when the *UBR1* gene is activated, the degron strain exhibits cell cycle arrest at the non-permissive temperature. Cells expressing the *ZePES*, *AtPES* and *NOP7/YPH1* cDNAs continued to grow at 37 °C, indicating functional complementation of the degron strain.

3.4. Subcellular localization of AtPES

To investigate the subcellular distribution pattern of AtPES, a *GFP*::*AtPES* fusion construct under the control of the *AtPES* promoter was generated. Since the NLS prediction of AtPES revealed the presence of three putative nuclear localization motifs, one at the N-terminal (residues 50–53) and two at the C-terminal end of the protein (residues 553–556 and 579–582), we decided to translationally fuse the entire cDNA to the *GFP* reporter gene. The subcellular localization of the GFP::AtPES fusion protein was examined in both *A. thaliana* cell suspension cultures and transgenic plants. As shown in Fig. 5a–c of the *A. thaliana* suspension cultures, AtPES–GFP fusion protein is localized almost exclusively at the nucleolus of the cells. The same distribution pattern was observed in transgenic plants, where the fusion protein was present at high levels in the nucleolus of the root epidermal cells (Fig. 5d–l).

3.5. Expression of AtPES during plant development

To compare the expression level of *AtPES* in different tissues and during early stages of development, semi-quantitative

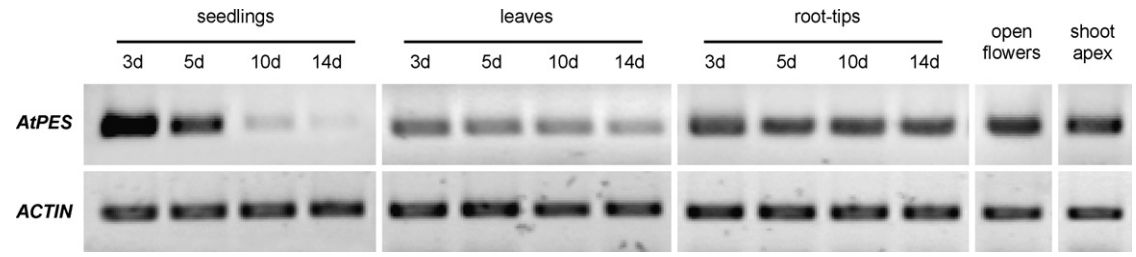

Fig. 6. RT-PCR analysis of *AtPES* gene expression. Semi-quantitative RT-PCR of steady state *AtPES* mRNA in different tissues and stages of *A. thaliana* (Col-0) development. Total RNA was prepared from seedlings, leaves, root-tips (3, 5, 10 and 14 days after germination), open flowers and 14-day-old shoot apices. Expression of the *ACTIN* gene was monitored as a control.

RT-PCR was employed using specific primers. Reverse transcription was conducted using RNAs extracted from *Arabidopsis* seedlings, leaves and root-tips at 3, 5, 10 and 14 days after germination (DAG), as well as from open flowers and 14-day-old shoot apices. As shown in Fig. 6, *AtPES* is expressed in all these tissues, with highest levels detected in young seedlings, root-tips, open flowers and shoot apices. Transcripts were high in 3-day-old seedlings but seemed to decline during development at 5, 10 and 14 DAG. Nevertheless, the constant expression level in the root-tip samples as well as the tissue specific *GUS* expression results (Fig. 7) indicate that this decrease in *AtPES* transcript levels is presumably due to the

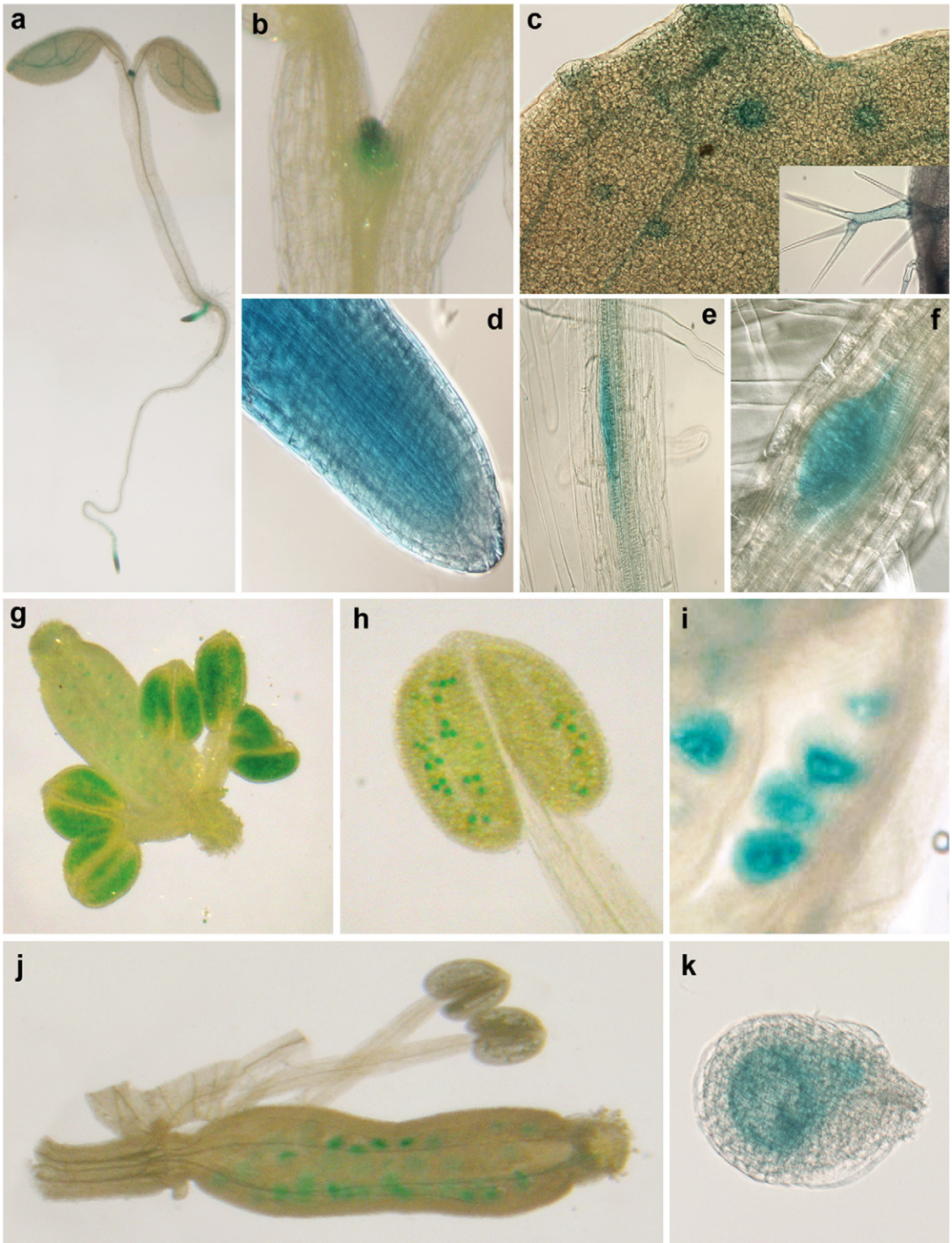

Fig. 7. Histochemical localization of *AtPES* promoter-GUS expression during vegetative and reproductive development of *A. thaliana*. (a–f) Representative expression pattern of *AtPES* expression in whole seedlings (a), shoot apices (b), young leaves (c), primary roots (d) and developing lateral roots (e and f). (g–k) Representative GUS staining pattern during flower development and fertilization, showing *AtPES* expression in immature pollen grains (g–h) and ovules (i–k).

ratio of the specific *AtPES* mRNA to total RNA from the entire seedling. Expression remained constant during leaf development, but transcript levels were lower than in other tissues. *AtPES* mRNA accumulation was also high in open flowers and 14-day-old shoot apices, suggesting a role of *AtPES* during both vegetative growth and reproductive development.

RT-PCR results only revealed the expression patterns of *AtPES* in major tissues. In order to investigate the tissue specific expression profile in more detail, a transgenic approach was chosen for the in planta characterization of *AtPES* promoter activity. Therefore, transgenic *Arabidopsis* plants were generated with a plasmid construct containing the *AtPES* promoter fragment linked to the *GUS* reporter gene (AtPESpro572GUS). A total of eight independent kanamycin-resistant transgenic lines were selected for the analysis of the reporter activity. All revealed similar GUS staining patterns, indicating that the selected promoter region is a functional unit. The constitutive promoter control (CaMV35S) showed strong GUS expression throughout the plants. No GUS activities were detected in the negative control transgenic plants containing a promoterless GUS construct (data not shown).

As shown in Fig. 7, the GUS staining patterns are consistent with the RT-PCR results. In young seedlings, strong *GUS* expression was detected in the shoot and root apical meristems (Fig. 7a, b and d) and moderate staining was observed in epidermal cells and the vascular tissue of the developing leaves (Fig. 7a and c). No expression was detected in mature leaves of flowering plants after 2 h of staining. However, a prolonged incubation for 24 h revealed minor staining of the vascular tissue. Significant GUS expression was also seen in trichome progenitor cells and during trichome development (Fig. 7c). Fig. 7e and f shows the *AtPES* regulated *GUS* expression at different stages of lateral root development. The staining was strongest in the pericycle-derived meristems as well as the entire emerging lateral root. In mature primary roots however, *GUS* expression was confined in the meristematic and early elongation zone (Fig. 7d) with little or no staining of the root-cap and the upper differentiation zone. During reproductive development and fertilization, *AtPES* expression was observed to be strong in young flowers (stages 12–15). Staining was prominent during micro- and macrosporogenesis with the most intense GUS activity observed in developing pollen grains and ovules (Fig. 7g–j). More detailed observation revealed that *AtPES* was expressed mainly in endosperm and the developing embryo of seeds at the preglobular and globular stages (Fig. 7k), and to a less extent in the integument tissue. In general, the above gene expression profile as well as the GUS staining pattern is consistent with the data from the publicly available *Arabidopsis* Microarray Database (GENEVESTIGATOR) [33].

3.6. Analysis of transgenic A. thaliana plants overexpressing AtPES

To test the effect of *AtPES* overexpression during plant development, we designed the construct pB35PES to overexpress the *AtPES* gene in *A. thaliana*. Overexpression of *AtPES* was determined in nine transgenic lines by semi-quantitative RT-PCR. However, all overexpressors displayed a wild-type root and shoot phenotype throughout development and no morphologically abnormal growth phenotypes were observed. Flower morphology, fertility and seed set were statistically similar to those from WT plants (data not shown). Thus, we suggest that overexpression of *AtPES* does not influence or alter the normal developmental program of *Arabidopsis*.

4. Discussion

In the present study, we report for the first time the isolation and characterization of the *pescadillo* orthologs from plants (*ZePES* from *Z. elegans* and *AtPES* from *A. thaliana*). The deduced amino acid sequences display high identity to the putative Pescadillo orthologs from rice and *Medicago* and less identity to orthologs from other species (Fig. 1). As visualized by the constructed phylogenetic tree, ZePES and AtPES are more closely related to the plant and lower eukaryotic sequences (which are clustered in one branch) than to the mammalian orthologs (Fig. 2). Both proteins contain, at similar positions, two distinct motifs (the pescadillo and BRCT domain), as well as a number of conserved consensus sequences for covalent attachment of SUMO-1 ubiquitin-related protein [30]. The convergence of function observed between proteins modified by SUMO-1 and proteins expressing a BRCT domain is consistent with the assigned role of Pescadillo as a key regulator of cell cycle progression. Ribosome biogenesis is a determinant of cell size, which is a requirement for cell division. In yeast, the association of Nop7/Yph1 with the origin of recognition complex (ORC) indicates, that Nop7/Yph1 action may directly link cell growth to cell division [14]. In the *Zinnia* mesophyl system, DAPI and Calcofuor staining reveals no cell divisions at time point 0 (non-inductive medium). However, 24 h after the addition of the hormones to the medium, about one-half (47%) of the cells have divided [32]. The elevated transcripts of *ZePES* in non-inductive medium indicate that the cells are probably at phase G1. Consistent with its putative role in preparing the cells to divide (ribosome biogenesis), *ZePES* expression is activated during G1/S (at 12 h) and G2/M (at 16 h) transition (Fig. 3). The expression pattern of the cell cycle genes is clearly delayed, if compared to that of sucrose-starved *Arabidopsis* suspension cultures (G1/S at 6 h and G2/M at 10 h) [34], or the auxin-mediated pericycle activation system (G1/S at 4 h and G2/M at 6 h) [35]. We presume that the observed delay (for 6–8 h), in activating the cell cycle machinery, is most likely due to the time the *Zinnia* mesophyll cells need to re-specify their fate and re-enter the cell cycle after hormonal perception.

Pescadillo seems to play a fundamental and evolutionarily conserved role. Considering the close phylogenetic relationship and the amino acid conservation of the pescadillo and BRCT domain between the plant and yeast Pescadillo orthologs, we asked whether ZePES and AtPES can substitute for yeast Nop7/Yph1 function. We show that both ZePES and AtPES are able to complement the thermosensitive phenotype of Y40047 on

galactose containing medium upon shifting cells from 24 to 37 °C (Fig. 4). Hence, the observed complementation of growth at non-permissive temperatures suggests both a structural and functional conservation of the protein function between yeast and plants.

The nucleolus is the most obvious and clearly differentiated nuclear subcompartment, and the site of synthesis and assembly of ribosome components. Although the fundamental processes of ribosome biogenesis are very similar in all eukaryotes, a number of reports indicate that some differences exist between plants and animals [36–40]. A proteomic analysis of the *Arabidopsis* nucleolus, for example, identified proteins with different localization between *Arabidopsis* and human [40]. Our results show that AtPES is imported into the nucleolus of plant cells and may therefore be involved in processes related to this compartment (Fig. 5). The subcellular localization of AtPES is consistent with results in yeast, who demonstrate that Nop7/Yph1 protein is required for the formation of $27SB_S$ rRNA [13].

AtPES displays a distinctive spatial expression pattern during plant development (Fig. 7). Analysis of transgenic plants harbouring a *AtPES*promoter::*GUS* fusion construct reveal that *AtPES* is predominantly expressed in highly proliferating tissues and actively dividing cells, where expression of ribosomal genes and genes encoding rRNA processing and ribosome assembly factors is a critical stage for cell proliferation and thus normal development. Interestingly, however, overexpression of *AtPES* does not lead to any phenotypic changes during growth and development. Significant GUS expression was also observed in trichome progenitor cells and developing trichomes. Leaf trichomes undergo successive endoreduplication rounds during development, in which chromosomal DNA is duplicated while cell division is arrested [41,42]. While endoreduplication has been associated with a cell-size increase in *Arabidopsis*, it is still unclear how nuclear DNA content can influence cytoplasmic growth. One mechanism by which this can be achieved is through controlling ribosome biogenesis [43]. However, trichomes are not the only cells which undergo endoreduplication. Plants are highly polysomatic, with endoreduplication events occurring in many other cells, such as root hair, hypocotyl and xylem cells, or in cell types that have high metabolic activity, such as endosperm and embryo suspensor cells [43,44]. It is therefore unclear whether *AtPES* expression in those tissues undergoing endocycles is correlated with the endoreduplication events *per se* or with the increased demand of new ribosomes to support macromolecular synthesis during cell growth.

Plant development requires stringent controls between cell proliferation and cell differentiation. Understanding the regulation and function of AtPES is critical to understanding the molecular bases of the existing and putative links between ribosome biogenesis, cell cycle progression, cell growth and cell fate specification.

Acknowledgments

Nicolas Tsesmetzis and co-workers are thanked for providing the pGreenII29+2X35S-GFP-35ST binary vector. The project is co-funded by the European Social Fund and National Resources (EPEAK II) PYTHAGORAS. MMcC was funded by a Royal Society University Research Fellowship.

References

[1] M.L. Allende, A. Amsterdam, T. Becker, K. Kawakami, N. Gaiano, N. Hopkins, Insertional mutagenesis in zebrafish identifies two novel genes, pescadillo and dead eye, essential for embryonic development, Genes Dev. 10 (1996) 3141–3155.
[2] J. Haque, S. Boger, J. Li, S.A. Duncan, The murine Pes1 gene encodes a nuclear protein containing a BRCT domain, Genomics 70 (2000) 201–210.
[3] Y. Kinoshita, A.D. Jarell, J.M. Flaman, G. Foltz, J. Schuster, B.L. Sopher, D.K. Irvin, K. Kanning, H.I. Kornblum, P.S. Nelson, P. Hieter, R.S. Morrison, Pescadillo, a novel cell cycle regulatory protein abnormally expressed in malignant cells, J. Biol. Chem. 276 (2001) 6656–6665.
[4] C.C. Adams, J. Jakovljevic, J. Roman, P. Harnpicharnchai, J.L. Woolford Jr., *Saccharomyces cerevisiae* nucleolar protein Nop7p is necessary for biogenesis of 60S ribosomal subunits, RNA 8 (2002) 150–165.
[5] E.V. Koonin, S.F. Altschul, P. Bork, BRCA1 protein products . . . functional motifs ..., Nat. Genet. 13 (1996) 266–268.
[6] P. Bork, K. Hofmann, P. Bucher, A.F. Neuwald, S.F. Altschul, E.V. Koonin, A superfamily of conserved domains in DNA damage-responsive cell cycle checkpoint proteins, FASEB J. 11 (1997) 68–76.
[7] I. Callebaut, J.P. Mornon, From BRCA1 to RAP1: a widespread BRCT module closely associated with DNA repair, FEBS Lett. 400 (1997) 25–30.
[8] M.S. Rodriguez, J.M. Desterro, S. Lain, C.A. Midgley, D.P. Lane, R.T. Hay, SUMO-1 modification activates the transcriptional response of p53, EMBO J. 18 (1999) 6455–6461.
[9] F. Melchior, SUMO-nonclassical ubiquitin, Annu. Rev. Cell Dev. Biol. 16 (2000) 591–626.
[10] F. Melchior, L. Hengst, Mdm2-SUMO1: is bigger better? Nat. Cell Biol. 9 (2000) 161–163.
[11] A. Lerch-Gaggl, J. Haque, J. Li, G. Ning, P. Traktman, S.A. Duncan, Pescadillo is essential for nucleolar assembly, ribosome biogenesis, and mammalian cell proliferation, J. Biol. Chem. 277 (2002) 45347–45355.
[12] Y.R. Lapik, C.J. Fernandes, L.F. Lau, D.G. Pestov, Physical and functional interaction between Pes1 and Bob1 in mammalian ribosome biogenesis, Mol. Cell 15 (2004) 17–29.
[13] M. Oeffinger, A. Leung, A. Lamond, D. Tollervey, Yeast Pescadillo is required for multiple activities during 60S ribosomal subunit synthesis, RNA 8 (2002) 626–636.
[14] Y.C. Du, B. Stillman, Yph1p, an ORC-interacting protein: potential links between cell proliferation control, DNA replication, and ribosome biogenesis, Cell 109 (2002) 835–848.
[15] A. Killian, N. Le Meur, R. Sesboue, J. Bourguignon, G. Bougeard, J. Gautherot, C. Bastard, T. Frebourg, J.M. Flaman, Inactivation of the RRB1-Pescadillo pathway involved in ribosome biogenesis induces chromosomal instability, Oncogene 23 (2004) 8597–8602.
[16] M. Prisco, A. Maiorana, C. Guerzoni, G. Calin, B. Calabretta, R. Voit, I. Grummt, R. Baserga, Role of pescadillo and upstream binding factor in the proliferation and differentiation of murine myeloid cells, Mol. Cell Biol. 24 (2004) 5421–5433.
[17] A. Maiorana, X. Tu, G. Cheng, R. Baserga, Role of pescadillo in the transformation and immortalization of mammalian cells, Oncogene 23 (2004) 7116–7124.
[18] A. Weber, U.R. Hengge, I. Stricker, I. Tischoff, A. Markwart, K. Anhalt, A. Dietz, C. Wittekind, A. Tannapfel, Protein microarrays for the detection of biomarkers in head and neck squamous cell carcinomas, Hum. Pathol. 38 (2007) 228–238.
[19] E.M. Sikorski, T. Uo, R.S. Morrison, A. Agarwal, Pescadillo interacts with the cadmium response element of the human heme oxygenase-1 promoter in renal epithelial cells, J. Biol. Chem. 281 (2006) 24423–24430.
[20] J. Mathur, L. Szabados, S. Schaefer, B. Grunenberg, A. Lossow, E. Jonas-Straube, J. Schell, C. Koncz, Z. Koncz-Kalman, Gene identification with sequenced T-DNA tags generated by transformation of *Arabidopsis* cell suspension, Plant J. 13 (1998) 707–716.

[21] C. Domingo, K. Roberts, N.J. Stacey, I. Connerton, F. Ruiz-Teran, M.C. McCann, A pectate lyase from *Zinnia elegans* is auxin inducible, Plant J. 13 (1998) 17–28.
[22] A. Sanchez-Diaz, M. Kanemaki, V. Marchesi, K. Labib, Rapid depletion of budding yeast proteins by fusion to a heat-inducible degron, Sci. STKE 223 (2004) l8.
[23] D. Mumberg, R. Müller, M. Funk, Yeast vectors for the controlled expression of heterologous proteins in different genetic backgrounds, Gene 156 (1995) 119–122.
[24] D. Becker, E. Kemper, J. Schell, R. Masterson, New plant binary vectors with selectable markers located proximal to the left T-DNA border, Plant Mol. Biol. 20 (1992) 1195–1197.
[25] G. An, P.R. Edbert, A. Mitra, S.B. Ha, Binary vectors, in: S.B. Gelvin, R.A. Shilperoort, D.P.S. Verma (Eds.), Plant Molecular Biology Manual, Kluwer Academic Publishers, Dordrecht, 1988, pp. 1–9.
[26] N. Bechtold, G. Pelletier, *In planta* Agrobacterium-mediated transformation of adult *Arabidopsis thaliana* plants by vacuum infiltration, Methods Mol. Biol. 82 (1998) 259–266.
[27] R.A. Jefferson, T.A. Kavanagh, M.W. Bevan, GUS fusions: beta-glucuronidase as a sensitive and versatile gene fusion marker in higher plants, EMBO J. 6 (1987) 3901–3907.
[28] D. Milioni, P.E. Sado, N.J. Stacey, K. Roberts, M.C. McCann, Early gene expression associated with the commitment and differentiation of a plant tracheary element is revealed by cDNA-amplified fragment length polymorphism analysis, Plant Cell 14 (2002) 2813–2824.
[29] X. Zhang, S. Morera, P.A. Bates, P.C. Whitehead, A.I. Coffer, K. Hainbucher, R.A. Nash, M.J. Sternberg, T. Lindahl, P.S. Freemont, Structure of an XRCC1 BRCT domain: a new protein–protein interaction module, EMBO J. 17 (1998) 6404–6411.
[30] D.A. Sampson, M. Wang, M.J. Matunis, The small ubiquitin-like modifier-1 (SUMO-1) consensus sequence mediates Ubc9 binding and is essential for SUMO-1 modification, J. Biol. Chem. 276 (2001) 21664–21669.
[31] X. Fu, C. Ng, D. Feng, C. Liang, Cdc48p is required for the cell cycle commitment point at Start via degradation of the G1-CDK inhibitor Far1p, J. Cell Biol. 163 (2003) 21–26.
[32] M. Mourelatou, J.H. Doonan, M.C. McCann, Transition of G1 to early S phase may be required for zinnia mesophyll cells to trans-differentiate to tracheary elements, Planta 220 (2004) 172–176.
[33] P. Zimmermann, M. Hirsch-Hoffmann, L. Hennig, W. Gruissem, GENEVESTIGATOR. Arabidopsis microarray database and analysis toolbox, Plant Physiol. 136 (2004) 2621–2632.
[34] M. Menges, J.A.H. Murray, Synchronous Arabidopsis suspension cultures for analysis of cell-cycle gene activity, Plant J. 30 (2002) 203–212.
[35] K. Himanen, E. Boucheron, S. Vanneste, J. de Almeida Engler, D. Inze, T. Beeckman, Auxin-mediated cell cycle activation during early lateral root initiation, Plant Cell 14 (2002) 2339–2351.
[36] P.J. Shaw, E.G. Jordan, The nucleolus, Annu. Rev. Cell Dev. Biol. 11 (1995) 93–121.
[37] M. Carmo-Fonseca, L. Mendez-Soares, I. Campos, To be or not to be in the nucleolus, Nat. Cell Biol. 2 (2000) E107–E112.
[38] P.J. Shaw, The Nucleolus. Nature Encyclopedia of Life Sciences, vol. 4, Nature Publishing Group, 2005, E0395802.
[39] K. Koberna, J. Malinsky, A. Pliss, M. Masata, J. Vecerova, M. Fialova, J. Bednar, I. Raska, Ribosomal genes in focus: new transcripts label the dense fibrillar components and form clusters indicative of ''Christmas trees'' in situ, J. Cell Biol. 157 (2002) 743–748.
[40] A.F. Pendle, G.P. Clark, R. Boon, D. Lewandowska, Y.W. Lam, J. Andersen, M. Mann, A.I. Lamond, J.W. Brown, P.J. Shaw, Proteomic analysis of the *Arabidopsis* nucleolus suggests novel nucleolar functions, Mol. Biol. Cell 16 (2005) 260–269.
[41] A. Schnittger, M. Hülskamp, Trichome morphogenesis: a cell-cycle perspective, Philos. Trans. R. Soc. Lond. 357 (2002) 823–826.
[42] M.L. Churchman, M.L. Brown, N. Kato, V. Kirik, M. Hulskamp, D. Inze, L. De Veylder, J.D. Walker, Z. Zheng, D.G. Oppenheimer, T. Gwin, J. Churchman, J.C. Larkin, SIAMESE, a plant-specific cell cycle regulator, controls endoreplication onset in *Arabidopsis thaliana*, Plant Cell 18 (2006) 3145–3157.
[43] K. Sugimoto-Shirasu, K. Roberts, ''Big it up'': endoreduplication and cell-size control in plants, Curr. Opin. Plant Biol. 6 (2003) 544–553.
[44] B.A. Larkins, B.P. Dilkes, R.A. Dante, C.M. Coelho, Y.M. Woo, Y. Liu, Investigating the hows and whys of DNA endoreduplication, J. Exp. Bot. 52 (2001) 183–192.